3D Finite-Element Analysis of Steel Moment Frames Including Long-Span Entrance by Strengthening Steel Cables and Diagonal Concentrically Braced Frames under Progressive Collapse

Amir Homaioon Ebrahimi, Ph.D.[1]; Mehdi Ebadi Jamkhaneh, Ph.D., Aff.M.ASCE [2]; and Maedeh Shokri Amiri[3]

Abstract: Progressive collapse in structures is considered a rare event. Yet, if it occurs, it may lead to disastrous human and financial loss. A significant item to study in examining progressive collapse relates to structures with relatively large spans. In such buildings, as the adjacent column collapses, maximum damage is caused to the entire structure. Therefore, in this study, six buildings of 16 and 31 m in height were, initially, subjected to nonlinear dynamic analysis upon the removal of a column. Shell elements were employed for concrete floors, and beam elements were used for beam members, columns, braces, and truss elements for cables, taking into account the nonlinear and geometric behavior of materials. The results of the numerical models were compared with the two experimental models, and a proper match was achieved. After the analysis of the primary structures, the two strengthening methods of braces and cables were employed by the removal of the column. The results of the study indicate that the use of cables and braces is able to significantly reduce the displacement of the node over the column by using an alternative-path method. Also, these two reinforcement methods are another reason for other structural elements to remain elastic. **DOI: 10.1061/(ASCE)SC.1943-5576.0000388.** *©2018 American Society of Civil Engineers.*

Author keywords: Progressive collapse; Steel moment frame; Nonlinear dynamic analysis; Cable; Diagonal concentrically braced frames.

Introduction

Since the explosion of a building in London on May 16, 1968, that resulted in the total collapse of part of the building, the assessment of existing structures upon the exertion of unusual, severe, and sudden loads (e.g., those caused by explosions, fires, aircraft impact, and terrorist attacks) has become a subject of interest for researchers and building designers aiming to prevent or at least reduce financial loss and human casualties. In conventional design methods, there usually are no regulations for such loads. In this phenomenon, the final destruction is not proportional to the initial damage, and this disproportion between the initial and the final situations has rendered a thorough analysis of this phenomenon complex. The occurrence of progressive collapse has already shown its consequences, and although rare, progressive collapse can cause irreparable damage to fundamental structures and those with special structural design or special uses. It must also be noted that, so far, no structural system that can completely manage the risks of progressive collapse has been introduced or employed, due to uncertainties inherent to design and the lack of a thorough understanding of the behavior of the system after its construction or of the materials used. Few design regulations and guidelines thoroughly address progressive collapse, and they mostly offer general tips for the reduction of the effects of this phenomenon. Among such regulations and guidelines are those by ASCE (2010), the DoD (2009), and the GSA (2013). The GSA (2013) guidelines include simplified analyses (regardless of the type of event) and examine the behavior of the structure after the removal of a vertical load-bearing element, taking into account the involved dynamic effects.

Recent years have witnessed extensive studies of the methods of damage reduction; for example, Galal and El-Sawy (2010) discussed the effect of retrofit strategies on mitigating the progressive collapse of steel frame structures. Following, Pirmoz and Liu (2016) discussed finite-element modeling and capacity analysis of posttensioned steel frames against progressive collapse. Homaioon Ebrahimi et al. (2017) analyzed the effect of plan irregularities on the progressive collapse of four steel structures located in regions with different seismic activity. They found that in most of the column-removal scenarios, an irregular structure designed in a Site Class C seismic zone would collapse. In addition, comparison of regular and irregular structures designed in a Site Class E seismic zone suggested that the ratio of demand force to capacity (D/C ratio) of the columns in the irregular structures is within the average range of 1.5 and 2 times the average D/C ratio of regular ones. Ebadi Jamkhaneh et al. (2015) did a nonlinear dynamic analysis of a six-floor special steel moment frame. To do so, they strengthened the steel moment frame with concentric braces and compared them with each other. Thy showed that under progressive collapse, there was a significant influence on the reduction of structural response.
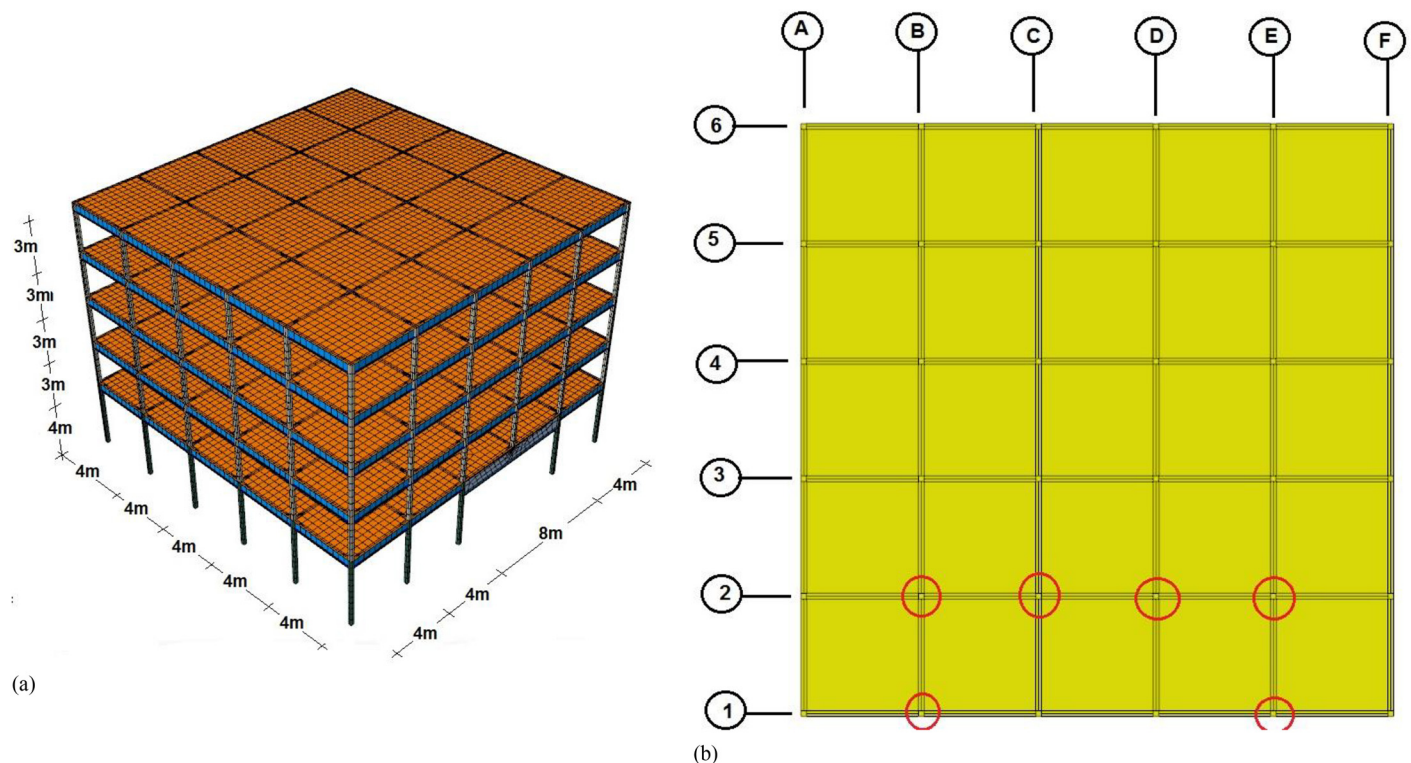
Kim et al. (2009) developed a system for the analysis of progressive collapse that, after assessing the damage in components, automatically creates a modified model for the next stage of analysis. Khandelwal et al. (2009) investigated the behavior of steel structures with concentrically and eccentrically braced frames (CBFs and EBFs, respectively) in progressive collapse. They found that moment frames with EBFs experienced less damage than those

[1]Graduate Student, School of Engineering, Univ. of Birmingham, Birmingham B15 2TT, UK. Email: homaioon.ebrahimi@yahoo.com

[2]Graduate Student, Faculty of Civil Engineering, Semnan Univ., Semnan 35131-1911, Iran (corresponding author). Email: mehdi.ebadi1985@hotmail.com

[3]Graduate Student, Islamic Azad Univ., Science and Research Branch, Tehran 14515/775, Iran. Email: maedeh.shokri@hotmail.com

© ASCE 04018025-1 Pract. Period. Struct. Des. Constr.

Pract. Period. Struct. Des. Constr., 2018, 23(4): 04018025

Fig. 1. Geometric dimensions and meshed model of all the elements in the five-story building: (a) 3D view; and (b) plan view.

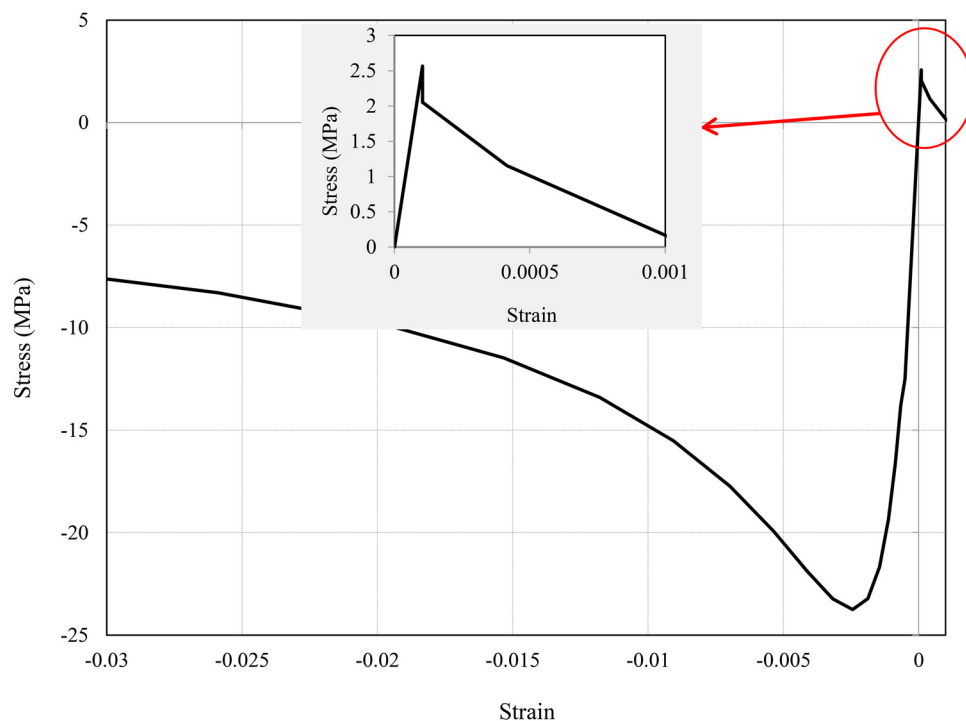**Table 1.** Geometric characteristics of beam and column sections

Story	Column	Beam
	5-story structure	
1	$HSS8 \times 8 \times 5/8$	$W21 \times 62$
2–5	$HSS8 \times 8 \times 3/8$	$W14 \times 30$
	10-story structure	
1–4	$HSS12 \times 12 \times 5/8$	$W21 \times 62$
5–8	$HSS10 \times 10 \times 3/8$	$W16 \times 40$
9–10	$HSS8 \times 8 \times 3/8$	$W14 \times 30$

Table 2. Mechanical characteristics of the steel

Characteristic	Value
Yield stress (MPa)	240
Ultimate stress (MPa)	370
Elastic modulus (MPa)	200,000
Yield strain (%)	0.19
Hardening strain (%)	1.7
Rupture strain (%)	3.2

with CBFs. Yet, design methods for the reduction of damage caused by progressive collapse are major challenges on which little research has been conducted. Lee et al. (2009) simplified the nonlinear progressive collapse analysis of welded steel moment frames. In addition, Naji and Irani (2012) conducted a progressive collapse analysis of steel frames, and they simplified the procedure and explicit expression for the dynamic increase factor. Liu (2010) employed optimization techniques to design structures with optimized costs and increased resistance to damage caused by progressive collapse. Gerasimidis and Sideri (2016), too, have conducted studies on the behavior of structures experiencing progressive collapse by offering a destruction method based on the column-removal technique. Kim and Kim (2009) employed the alternative-path technique to assess the capacity of resistance to collapse, using DoD (2009) and GSA (2013) guidelines, in structures under static and dynamic loads. They found that the structural response in dynamic analysis was greater than that in static analysis and that the results will depend on such parameters as the magnitude of the load, the location of the removed column, and the number of floors. Kwasniewski (2010) investigated the effect of simulation parameters in the progressive collapse caused by fire in the Cardington
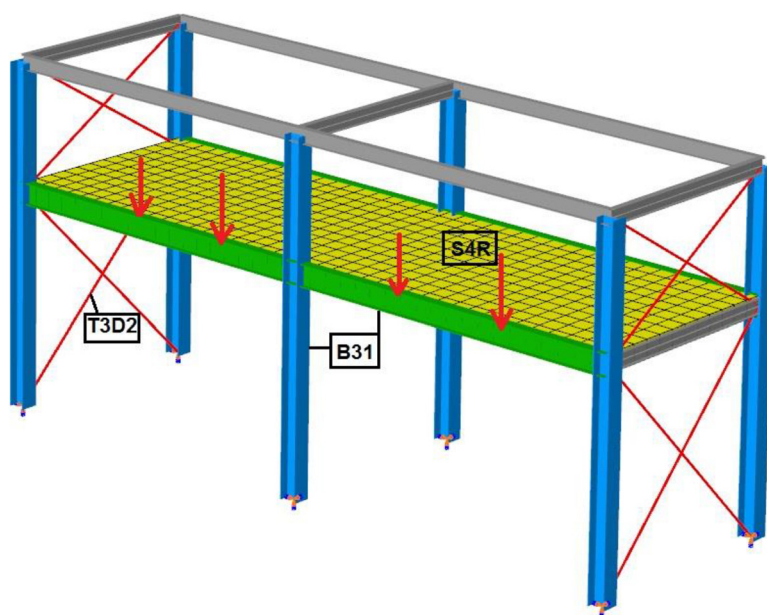
Large Building Test Facility upon the removal of columns at three locations in the building, using three-dimensional (3D) simulation. Kwasniewski (2010) found that the likelihood of structural collapse in the three assumed scenarios was quite low. Elsanadedy et al. (2014) investigated the effect of explosion on progressive collapse in a six-story steel structure with moment frames. They found that limiting the access distance with the peripheral columns reduced the likelihood of destruction upon explosion and that for the reduction of the damage, the structure should be strengthened with systems such as steel plate shear walls and diagonal CBFs. Gerasimidis (2014) investigated the removal of corner columns (independent of the cause of the removal) in regular and irregular steel frames and examined the effects of the number of floors and of irregularity on progressive collapse. Gerasimidis (2014) found that the location of the removed column on different floors was associated with different progressive collapse mechanisms. The removal of columns on lower floors resulted in yield and damage to columns in the floors above the location of the removed column, leading to flexural failure of the beams. Galal and El-Sawy (2010) employed the alternative-path method to investigate the effects of improving the techniques for reinforcing beam strength, increasing beam stiffness, and simultaneously increasing beam stiffness and strength on the reduction of

© ASCE

04018025-2

Pract. Period. Struct. Des. Constr.

Pract. Period. Struct. Des. Constr., 2018, 23(4): 04018025

**Fig. 2.** Stress-strain curve of the concrete used in the floors.

Fig. 3. Support conditions, types of structural elements, and locations of load exertion as simulated in the finite-element model using *Abaqus* and in accordance with Wang et al. (2007).

the effects of progressive collapse in steel structures with moment-frame systems. They found that in all the scenarios based on DoD (2009) guidelines, collapse was inevitable, and increasing the beam capacity had a bigger effect on the improvement of the indices in question than that of increasing beam stiffness. Pirmoz and Liu (2016), by investigating progressive collapse in steel frames with posttensioned strands, showed that beam arching action and strand catenary action are major contributors to the capacity of the posttensioned steel frame against progressive collapse. Fu et al. (2016)

investigated the dynamic behavior of steel structures with bolted-angle steel joints upon column removal using the alternative-path method. In this study, the dynamic increase factor was calculated by comparing the dynamic behavior with the nonlinear static behavior of the joint, and the results showed that the numerical method yielded reasonable matches with the results of the energy-balance method. Rezvani et al. (2015) investigated the effect of reducing the span length to half of the initial length and showed that the capacity upon the removal of middle columns significantly increased, and
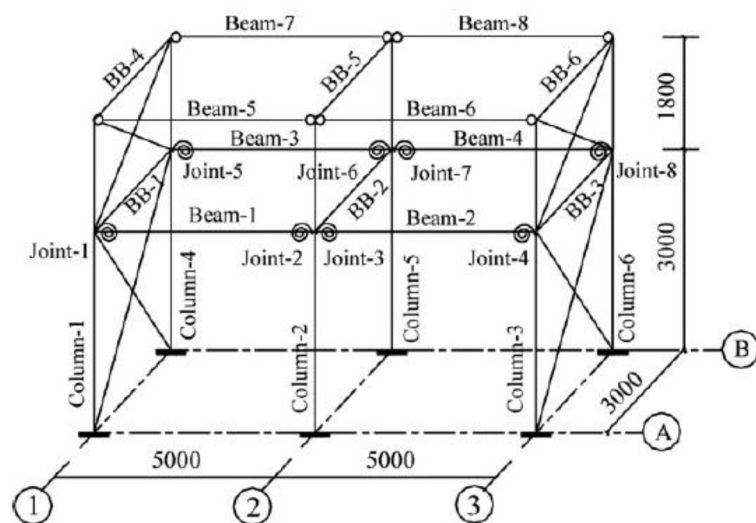
Fig. 4. Detail and dimensions of the experimental sample. (Data from Wang et al. 2007.)

Table 3. Mechanical characteristics of structural elements

Specimen	Yield strength (MPa)	Ultimate strength (MPa)	Elongation at fracture (%)
Steel beam flange	304.3	438.6	34.6
Steel beam web	304.8	460.9	33.0
Steel column flange	301.6	463.1	30.9
Steel column web	289.3	457.7	31.0

Table 4. Geometric characteristics of structural elements

Specimen	Height (mm)	Width of flange (mm)	Flange thickness (mm)	Web thickness (mm)
Column	250	250	14	9
Beams 1–4	300	150	9	6.5
BBs 1–6 and Beams 5–8	200	100	8	5.5

with increased exerted loads, the likelihood of progressive collapse due to the removal of middle columns increased.

To prevent the failure behavior of steel structures, there are some innovative passive-control systems that can improve the stability of high rise buildings in extreme earthquakes by preventing the buckling of bracing systems and dissipation of earthquake energy in a circular element (Bazzaz et al. 2011, 2012a, b, 2014, 2015a, b, Andalib et al. 2014).
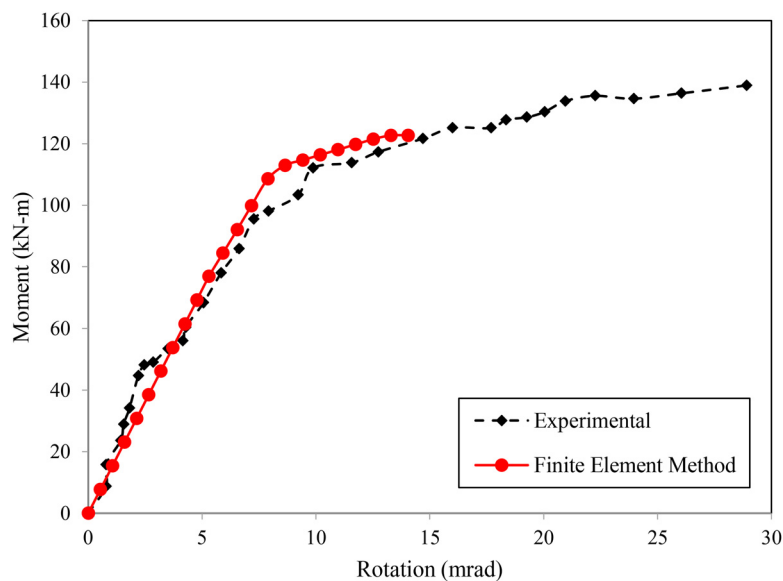
One of the challenges that designers face when designing commercial buildings is the necessity of ample space for the building entrance. One solution to this problem is the removal of one of the columns on the first floor to create this space. One potential risk associated with the removal of a column and creating a large span is the failure of one or both adjacent columns, which can lead to local instability and, if unconsidered in the design, can lead to significant damage. The present study focused on investigating the occurrence of the removal of one of the adjacent columns on either side of a long span in low- and midrise structures along with two strengthening methods: (1) the use of diagonal concentric braces at the top of the long span where a column has been removed and (2) the use of cables in the first and second stories to

resist against the progressive collapse. These scenarios have not received adequate attention from scholars. In this study, analysis of six steel structures of 5 and 10 stories in height was conducted using nonlinear dynamic analysis.
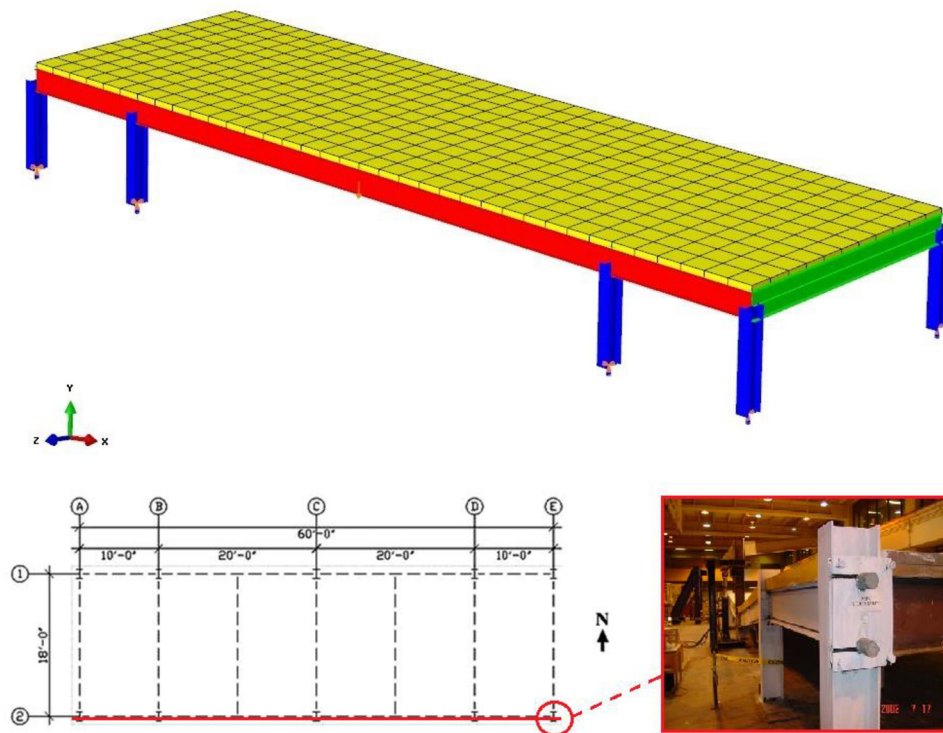
Geometric and Mechanical Characteristics

In this study, the finite-element analysis software *Abaqus 6.14* was employed to model the samples. A 3D integrated finite-element model of 5- and 10-story structures with moment-resisting frames is shown in Fig. 1. These structures were first designed using ETABS according to ASCE (2010) and AISC (2010) guidelines. The structures of the designed buildings were perfectly symmetrical in two horizontal directions, and they had five 4-m spans; each floor had a height of 3 m (except the fourth floor, which was 4 m high). Table 1 shows the geometric characteristics of the beam and column sections. It should be noted that beam–column connections were modeled as fully rigid joints, and the beam section only at the entrance, on the first floor, is of the type $W\,40 \times 149$. Dead and live loads were identical on all floors at 3.9 and 3.17 kN·m², respectively. A bilinear model was used for the steel material, consisting of a linear elastic phase and a post-yield linear hardening phase with stiffness equal to 2–3% of the initial stiffness. A von Mises yield surface was considered for this steel material. Young's modulus was 200 GPa, the Poisson's ratio was 0.3, and the density was 7,800 kg/m³. Table 2 outlines the characteristics of the steel used in the beams and columns.

Concrete damage plasticity is the only model that can be used in both nonlinear static and nonlinear dynamic analyses in *Abaqus*. In this study, Nayal and Rashid's (2006) model was used to plot the stress-strain ratio at the tension area. The model proposed by Hsu and Hsu (1994) was used to plot the compressive stress-strain ratio of the concrete. Fig. 2 shows the stress-strain curve of the concrete used in this study, where the compressive and tensile strengths of the concrete were assumed at 23 and 2.5 MPa, respectively, and the volumetric mass density of the concrete was assumed as 2,350 kg/m³. The cables used in this study were composed of several cables, and the overall diameter of the wire twisted together was assumed as 100 mm. In this software, cables have a circular section and are of elastoplastic materials. The Poisson's ratio of the cable was assumed as 0.3.

© ASCE 04018025-4 Pract. Period. Struct. Des. Constr.

Pract. Period. Struct. Des. Constr., 2018, 23(4): 04018025

Fig. 5. Bending moment–rotation curve at Node 1 in experimental and numerical samples.

Fig. 6. Plan and detail of finite-element and experimental models reinforced with steel cables. (Data from Tan and Astaneh-Asl 2003.)

Characteristics of Elements Used in Modeling

Beam and column elements were Type B31, and floor roofs were modeled using shell elements S4R. B31 is a shear flexible with linear interpolation. S4R is a reduced-integration quadrilateral shell element considering shear deformation and is applicable to large-strain deformation. A fine mesh was used for the beam-to-column

Table 5. Geometric characteristics of structural elements

Specimen	Height (mm)	Width of flange (mm)	Flange thickness (mm)	Web thickness (mm)
W14 × 61	353	254	16.4	9.5
W21 × 44	525	165	11.4	8.9
W18 × 35	450	152	10.8	7.6

© ASCE 04018025-5 Pract. Period. Struct. Des. Constr.

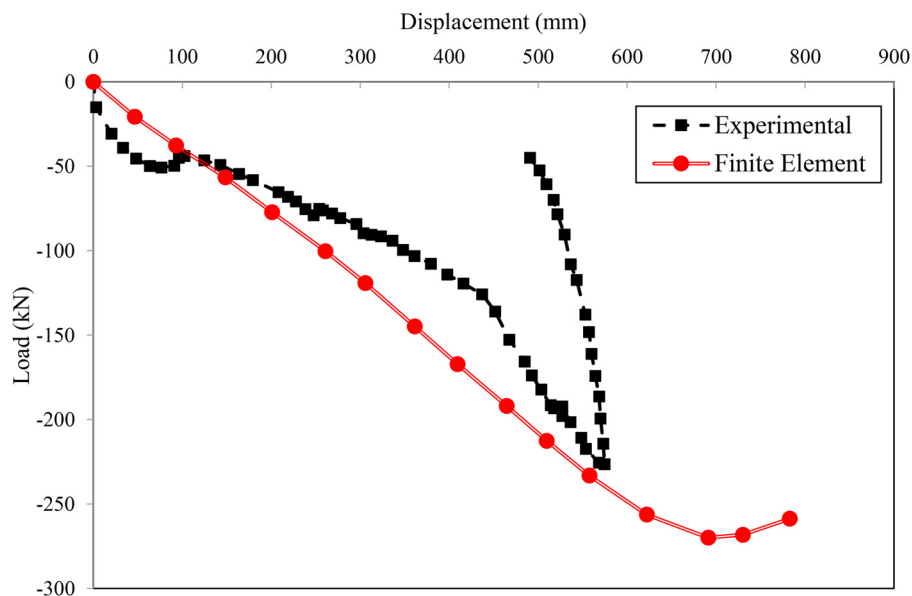Pract. Period. Struct. Des. Constr., 2018, 23(4): 04018025

Fig. 7. Force-displacement curve in laboratory and numerical models.

Table 6. Criteria for the acceptability of steel connections in nonlinear analyses

Section	A	B	C	Plastic rotation angle (rad)
$W21 \times 62$	0.0304	0.02	0.2	0.0304
$W14 \times 30$	0.0346	0.0228	0.2	0.0346

connections and column bases. In other parts, coarse meshing was used to reduce the analysis time. Because cable elements can only tolerate tensile forces and can tolerate no compressive forces and because they have axial stiffness, truss elements were employed. The total number of elements and nodes in the five-story structure were 10,268 and 10,529, respectively. Reinforcement was represented in each shell element by defining the area of reinforcement at the appropriate depth of the cross section using the *REBAR element from the *Abaqus* library. This reinforcement was defined in both slab directions and was assumed to act as a smeared layer. The reinforcement was modeled using the same elastic-plastic model as the main structural steel members.

From a geometric viewpoint and in regard to material behavior, the response of either the elements or the structure to abnormal loading conditions is most likely to be dynamic and nonlinear. Therefore, analytical methods that are necessary for the determination of the response of the structure must represent the sudden application of the abnormal loading, the dynamic behavior of the materials under very high strain rates, the inelastic postdamage behavior of the materials, and the geometric nonlinearity resulting from large deformations.

Under high loading rates, RC structures are expected to have a different response from the scenario of static loading. As an example, concrete shows a strongly rate-dependent behavior because compressive and tensile strengths are significantly correlated with strain rate (FIB 2008; Bischoff and Perry 1991). This is supported by experimental tests carried out through Split Hopkinson Bar (Grote et al. 2001). As Malvar and Crawford (1998) suggested, the International Federation for Structural Concrete (FIB 2008) describes the rate-dependent behavior of concrete in compression by means of a rate-dependent modulus of elasticity and the dynamic increase factors (DIFs) on strength. The estimation of the effect of strain rate on Young's modulus and the dynamic increase factors is done as follows:

$$\frac{E_c}{E_{c,\text{st}}} = \left(\frac{\dot{\varepsilon}}{\dot{\varepsilon}_{\text{st}}}\right)^{0.026} \tag{1}$$

$$\frac{f_c}{f_{c,\text{st}}} = \begin{cases} \left(\dfrac{\dot{\varepsilon}}{\dot{\varepsilon}_{\text{st}}}\right)^{1.026\alpha_s} & \text{for } \dot{\varepsilon} \leq 30 \text{ s}^{-1} \\[2mm] \gamma_s \left(\dfrac{\dot{\varepsilon}}{\dot{\varepsilon}_{\text{st}}}\right)^{1/3} & \text{for } \dot{\varepsilon} \geq 30 \text{ s}^{-1} \end{cases} \tag{2}$$

where E_c = compressive Young's modulus at strain rate $\dot{\varepsilon}$; $E_{c,\text{st}}$ = compressive static Young's modulus; f_c = compressive strength at strain rate $\dot{\varepsilon}$; $f_{c,\text{st}}$ = static compressive strength; $\dot{\varepsilon}$ = strain rate between 0.00003 and 300 s^{-1}; $\dot{\varepsilon}_{\text{st}}$ = compressive static strain rate of 0.00003 s^{-1}; and $\log(\gamma_s) = 6.156 \times \alpha_s - 2$; $\alpha_s = 1/(5 + 9f_{c,\text{st}}/10^7)$.
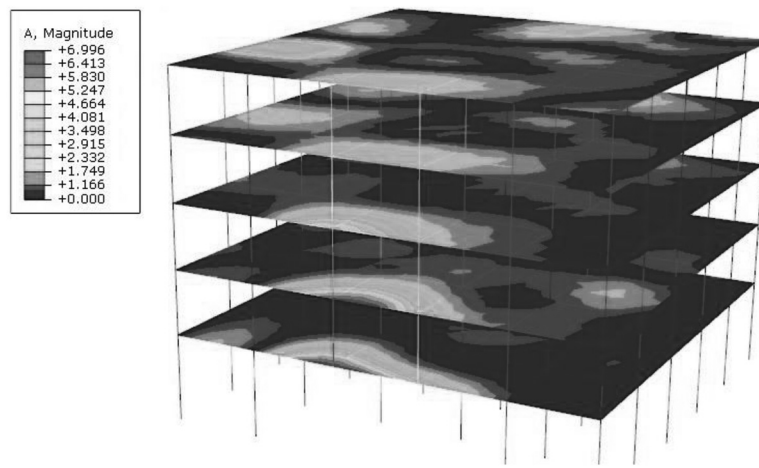
The tensile behavior of concrete is also rate dependent. As introduced by FIB (2008), the expression for the rate dependence of Young's modulus and the tensile strength is

$$\frac{E_t}{E_{t,\text{st}}} = \left(\frac{\ddot{\varepsilon}}{\ddot{\varepsilon}_{\text{st}}}\right)^{0.026} \tag{3}$$
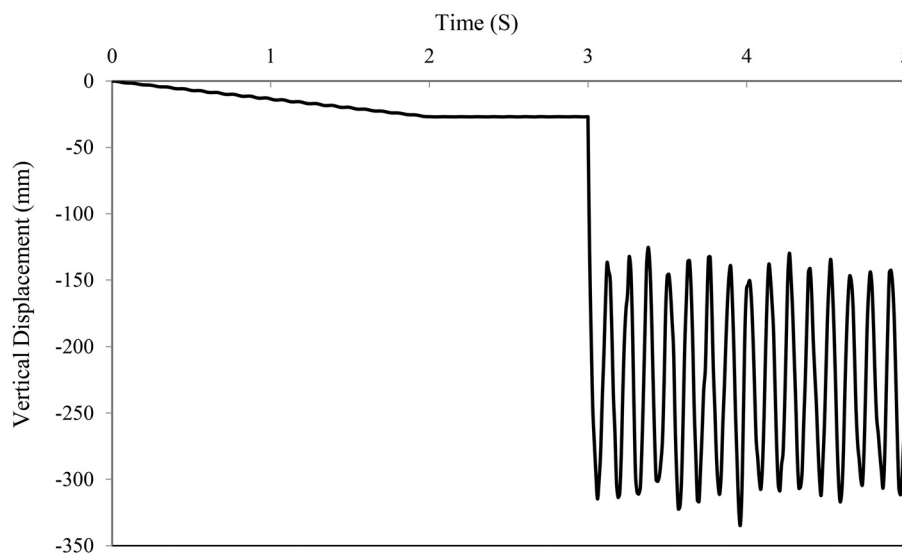
$$\frac{f_t}{f_{t,\text{st}}} = \begin{cases} \left(\dfrac{\ddot{\varepsilon}}{\ddot{\varepsilon}_{\text{st}}}\right)^{1.016\delta_s} & \text{for } \ddot{\varepsilon} \leq 30 \text{ s}^{-1} \\[2mm] \beta_s \left(\dfrac{\ddot{\varepsilon}}{\ddot{\varepsilon}_{\text{st}}}\right)^{1/3} & \text{for } \ddot{\varepsilon} > 30 \text{ s}^{-1} \end{cases} \tag{4}$$

where E_t = tensile Young's modulus at strain rate $\ddot{\varepsilon}$; $E_{t,\text{st}}$ = tensile static Young's modulus; f_t = tensile strength at strain rate $\ddot{\varepsilon}$; $f_{t,\text{st}}$ = static tensile strength; $\ddot{\varepsilon}$ = strain rate between 3×10^{-6} and 300 s^{-1}; $\ddot{\varepsilon}_{\text{st}}$ = tensile static strain rate of 3×10^{-6} s^{-1}; and $\log(\beta_s) = 7.11 \times \delta_s - 2.33$; $\delta_s = 1/(10 + 6f_{c,\text{st}}/10^7)$.

Malvar and Crawford (1998) suggested that in the case of steel, Young's modulus is assumed to be rate independent. The rates corresponding to the yield stress and the ultimate stress for steel follow the following expressions:

© ASCE   04018025-6   Pract. Period. Struct. Des. Constr.

Pract. Period. Struct. Des. Constr., 2018, 23(4): 04018025

Fig. 8. Acceleration contour for an unreinforced five-story structure.

Fig. 9. Curve of the displacement above the removed column.

$$\frac{f_y}{f_{y,\text{st}}} = \left(\frac{\varepsilon'}{\varepsilon'_{\text{st}}}\right)^{\alpha_y} \tag{5}$$

$$\frac{f_u}{f_{u,\text{st}}} = \left(\frac{\varepsilon'}{\varepsilon'_{\text{st}}}\right)^{\alpha_u} \tag{6}$$

where f_y = yield stress at strain rate ε'; $f_{y,\text{st}}$ = static yield stress; f_u = ultimate stress at strain rate ε'; $f_{u,\text{st}}$ = static ultimate stress; ε' = strain rate between $10^{-4}\,\text{s}^{-1}$ and $225\,\text{s}^{-1}$; ε'_{st} = static strain rate of $10^{-4}\,\text{s}^{-1}$; $\alpha_y = 0.074 - 0.040 f_y/414$; and $\alpha_u = 0.019 - 0.009 f_y/414$.
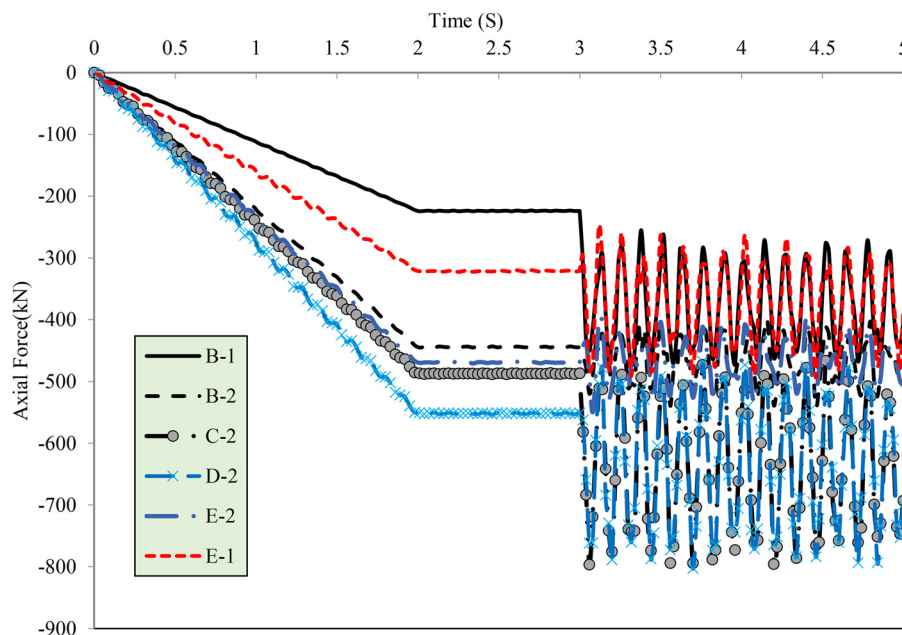
Validation of the Model

To ensure the accuracy of modeling technique in this study, validation of the numerical model was conducted in two parts. In the first part, the laboratory study of Wang et al. (2007)

was employed for modeling the cross braces. In the second part, the modeling of cables in frames according to the experimental studies of Tan and Astaneh-Asl (2003) was examined and validated.

Part 1

To ensure the accuracy of the proposed model, a two-story steel frame with composite floor was simulated in *Abaqus* (Fig. 3). This model was based on the laboratory study by Wang et al (2007) (Fig. 4). The height of the first floor was 3 m, and that of the second floor was 1.8 m. The frame featured two 5-m spans along the length and a 3-m span along the width. The ends of columns/beam were assumed as fully rigid, and two concentrated loads were exerted on Frame A at distances of one-third of the span length. First, force was applied monotonically in five stages to reach 170 kN, and then it was increased in 15-kN increments until one of the beams yielded. For braces, bars of 10 mm in diameter, yield tension of

© ASCE 04018025-7 Pract. Period. Struct. Des. Constr.

Pract. Period. Struct. Des. Constr., 2018, 23(4): 04018025

Fig. 10. Curve of the internal axial force in the columns around the removed column on the ground floor.
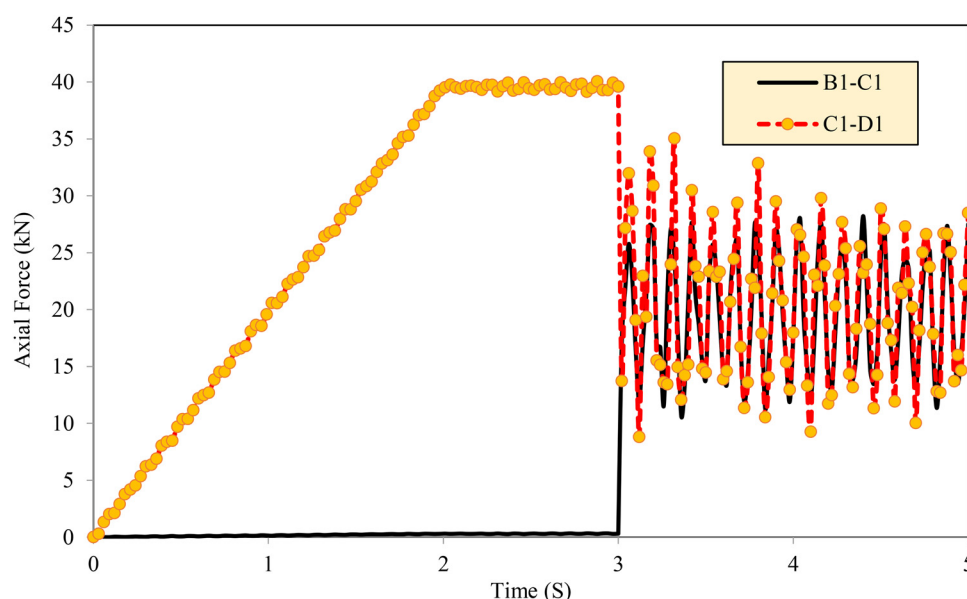
Fig. 11. History of the internal axial force in the columns around the removed column on the ground floor.
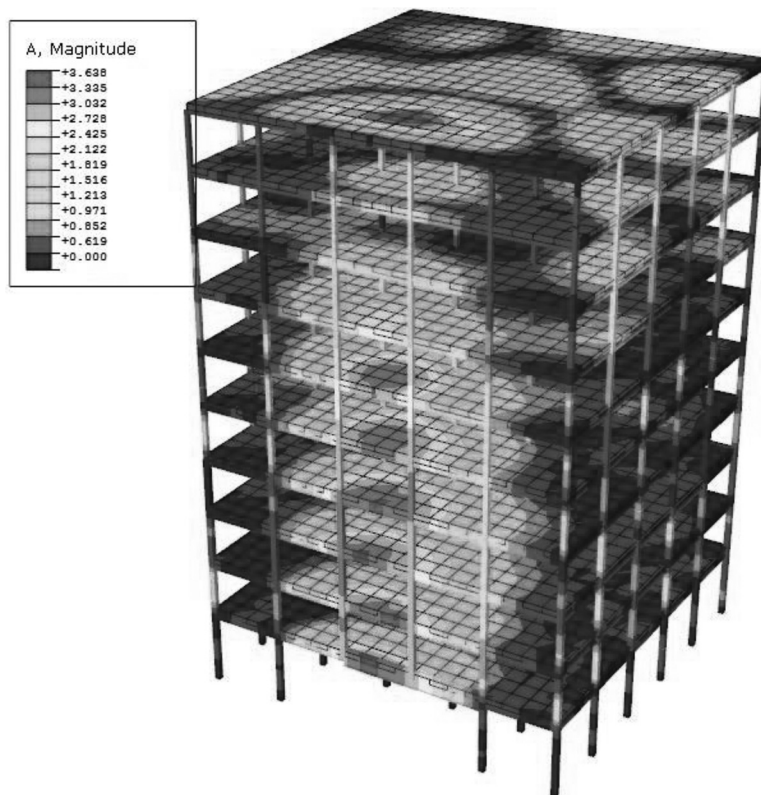
377.5 MPa, and a final strain of 29.7% were used. In the modeling of beams and columns, B31 was used; in that of braced element, T3D2; and in that of concrete slabs, S4R, as previously explained. The total number of elements was 760. The connections between the slab surface and structural beams with tie constraints were used. Tables 3 and 4, respectively, outline the mechanical and geometric characteristics of the steel of the elements of the reference sample. Fig. 5 compares the results of the bending moment–rotation at Node 1. In the comparison of laboratory and numerical results, reasonable accuracy was seen in the linear and nonlinear stages. Thus, the modeling technique, induced boundary condition, and other

assumptions can be valid in modeling structural elements, such as beams, columns, braces, and concrete shell floors.
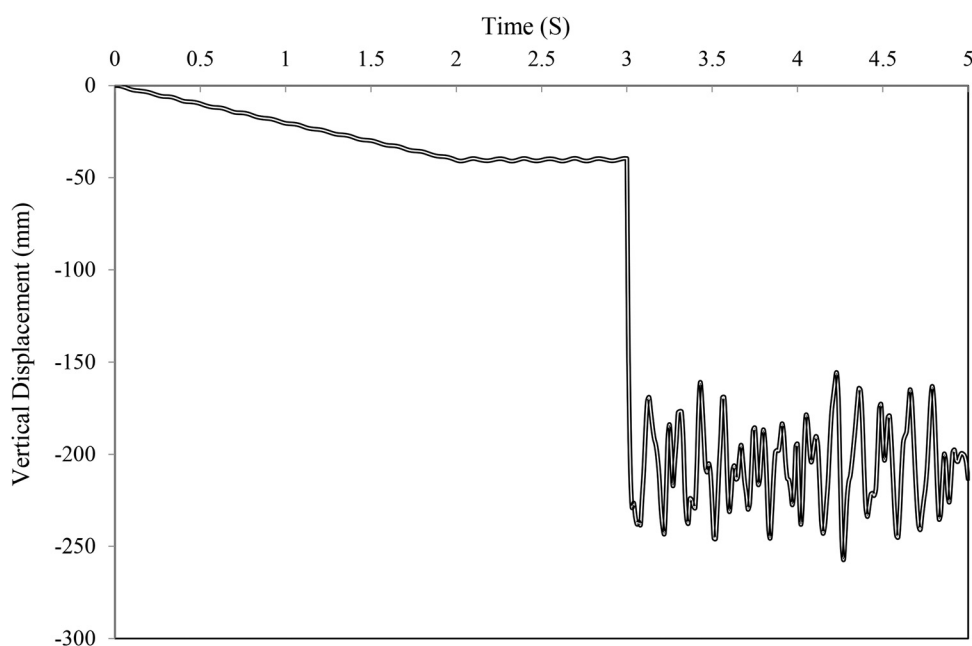
Part 2

To ensure the accuracy of the cable modeling, the experimental model Tan and Astaneh-Asl (2003) was used. The model was a moment-resisting frame for a one-story building with a concrete slab, with four spans along the length and one span along the width. As shown in Fig. 6, the model was 6,100 mm wide and 18,300 mm long. The final height of the concrete slab was 1,900 mm. The beams along the length had a section of $W\,18 \times 35$; the beams along

© ASCE — 04018025-8 — Pract. Period. Struct. Des. Constr.

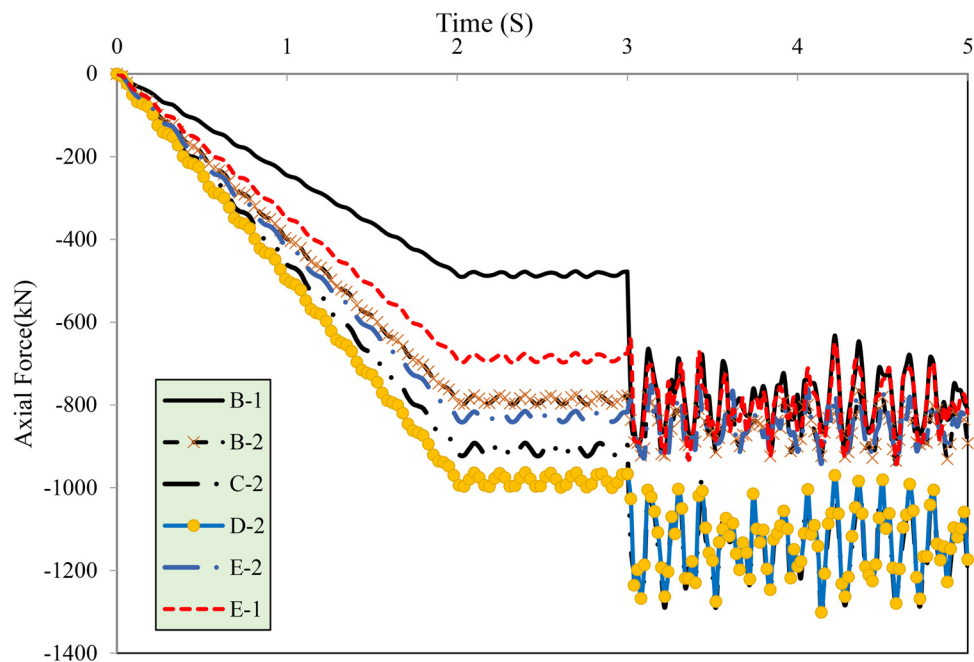Pract. Period. Struct. Des. Constr., 2018, 23(4): 04018025

**Fig. 12.** Acceleration contour for an unreinforced 10-story structure.

Fig. 13. Curve of the displacement above the removed column.

the width, $W\,21 \times 44$; and the columns, $W\,14 \times 61$. Table 5 shows the dimensions of these sections. The yield stress of all steel sections was assumed as 248 MPa, and concrete compressive strength was assumed as 28 MPa. In this experiment, two strong ASTM A586 cables of 19 mm in diameter and 18,700 mm in length were used. The rupture stress of the cables was assumed as 1,520 MPa,

and the elasticity modulus was assumed as 165 MPa. The loading rate was a displacement of 6 mm per second. The model pushed the column down up to a 560-mm vertical displacement. To consider the pin joints between beams and columns, U-joints with rotation capability between the nodes of the two ends of the beams and columns were employed. Also, to simplify the analysis, a T3D2 cable

© ASCE 04018025-9 Pract. Period. Struct. Des. Constr.

Pract. Period. Struct. Des. Constr., 2018, 23(4): 04018025

Fig. 14. Curve of the internal axial force in the columns around the removed column on the ground floor.
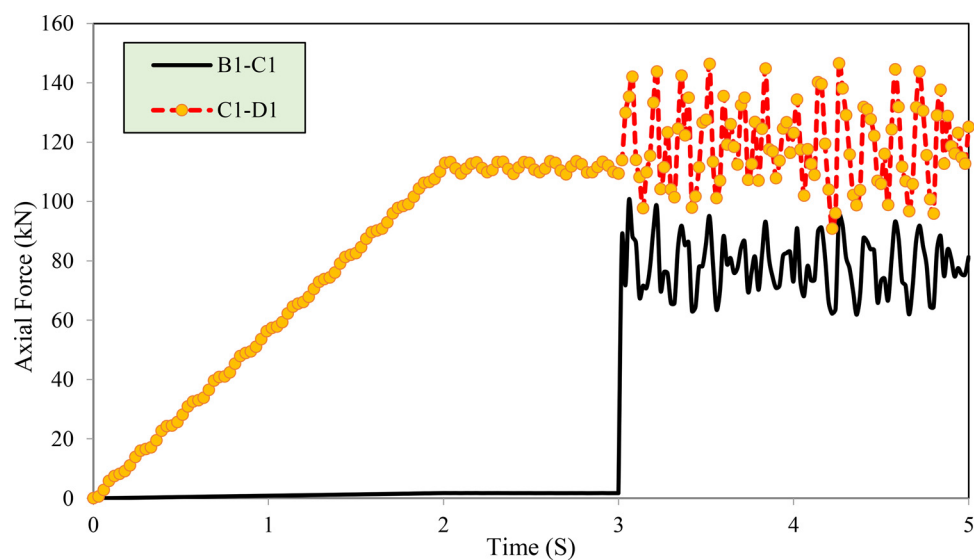
Fig. 15. History of the internal axial force in the columns around the removed column on the ground floor.

with a section of 567 mm^2 was fixed at the edge of the southern plan with tie constraints so that cable support was simulated. Fig. 7 shows a slight discrepancy in the initial stiffness trend between the finite-element and experimental models, but because the objective was to examine progressive collapse, this precision can be used in modeling, and simple assumptions can be used to apply the ties in the finite-element modeling of structures.

Loading Trend and Proposed Strengthening Models

In this study, the alternative-path method (APM) recommended by the GSA (2013) guidelines was employed. The progressive collapse in two 5- and 10-story buildings and the ways of counteracting it

were investigated. As outlined in the GSA (2013) guidelines, the overall methodology was to use the column-removal scenario to assess the strength of the structure against progressive collapse. In severe events such as explosion and impact, the dynamic effects exerted are independent of the event. The sudden-column-removal scenario is a suitable scenario for designing structures resistant to progressive collapse. This scenario is not similar to the dynamic effects of column failure due to impact or explosion; nonetheless, this scenario can, in a short time, give the effect of yield and column destruction on the structural response. Thus, sudden column loss is the principal design scenario in the guidelines. Also, for most designers, it is important that they make the structure resistant to progressive collapse upon the removal of a critical column. Therefore, the capacity of the structure upon sudden column
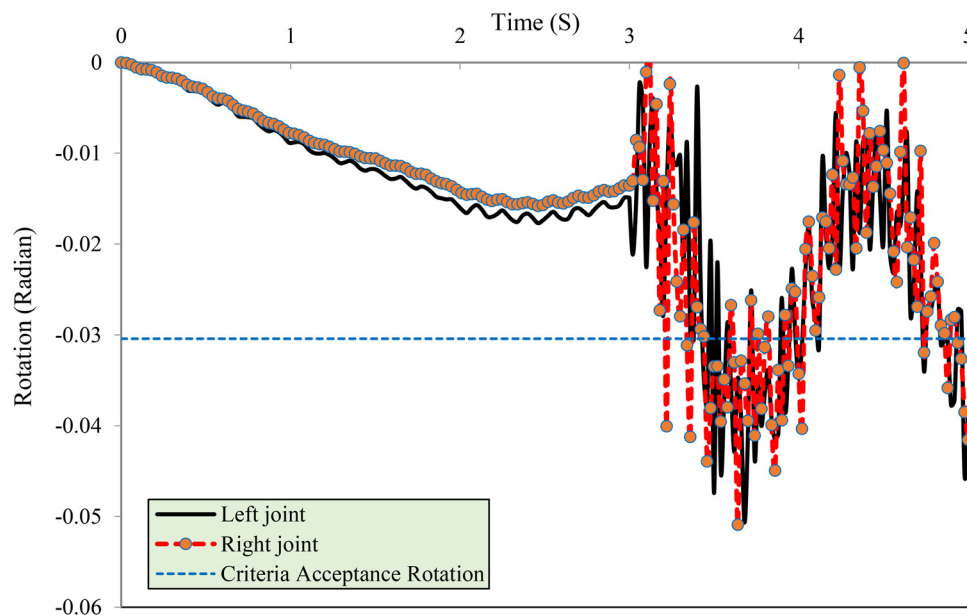
© ASCE 04018025-10 Pract. Period. Struct. Des. Constr.

Pract. Period. Struct. Des. Constr., 2018, 23(4): 04018025

Fig. 16. History of plastic rotation in Beam B1-C1 around the removed column on the ground floor.

removal can be investigated through nonlinear dynamic analysis using the 3D finite-element technique.

Following the GSA (2013) guidelines, load combinations including 120% of dead load plus 50% of the total live load were gradually applied within a time frame of 2 s. Then, to account for nonlinear dynamic effects, the load was maintained steadily for the following 1 s. After the 3-s sequence, when gravity load effects were considered to be fully transferred to the structure, a preselected column was suddenly removed from the model, and the structural response was examined. Another point to be noted is that in dynamic analysis with *Abaqus*, the column cannot be removed. Therefore, in this case, by changing the boundary conditions of the support of the column (full degree freedom of the column support), column removal was simulated. In accordance with Table 5.2 of the GSA (2013) guidelines, the criteria for the acceptability of primary and secondary steel elements in nonlinear analyses for fully rigid connections are given in Table 6.

Results of Numerical Models

Five-Story Structure with Moment-Resisting Frames

When Column C1 (Fig. 8) was suddenly removed, the node above the removed column started to vibrate and reached a maximum displacement of 335 mm. The final response of the structure equaled 246 mm (Fig. 9). The beam and the adjacent column were initially put under severe loading and start to undergo inelastic deformation. Fig. 10 shows the ensuing large redistribution of the force. The maximum force resulting in columns around the removed column belonged to C2, which experienced a 63% growth, from 486 to 797 kN. Nonetheless, the maximum rate of increase in the force (112%) belonged to Column B1, which was adjacent to the removed column. As shown in Fig. 11, the force in Beam B1-C1 reached a maximum of 28.2 kN before rising to the final magnitude of 25 kN. The rest of the structural elements remained elastic. The most critical column in this structure was the removed column because, upon its removal, a large area of loading was left without a column, and because of the removal of the column, part of the
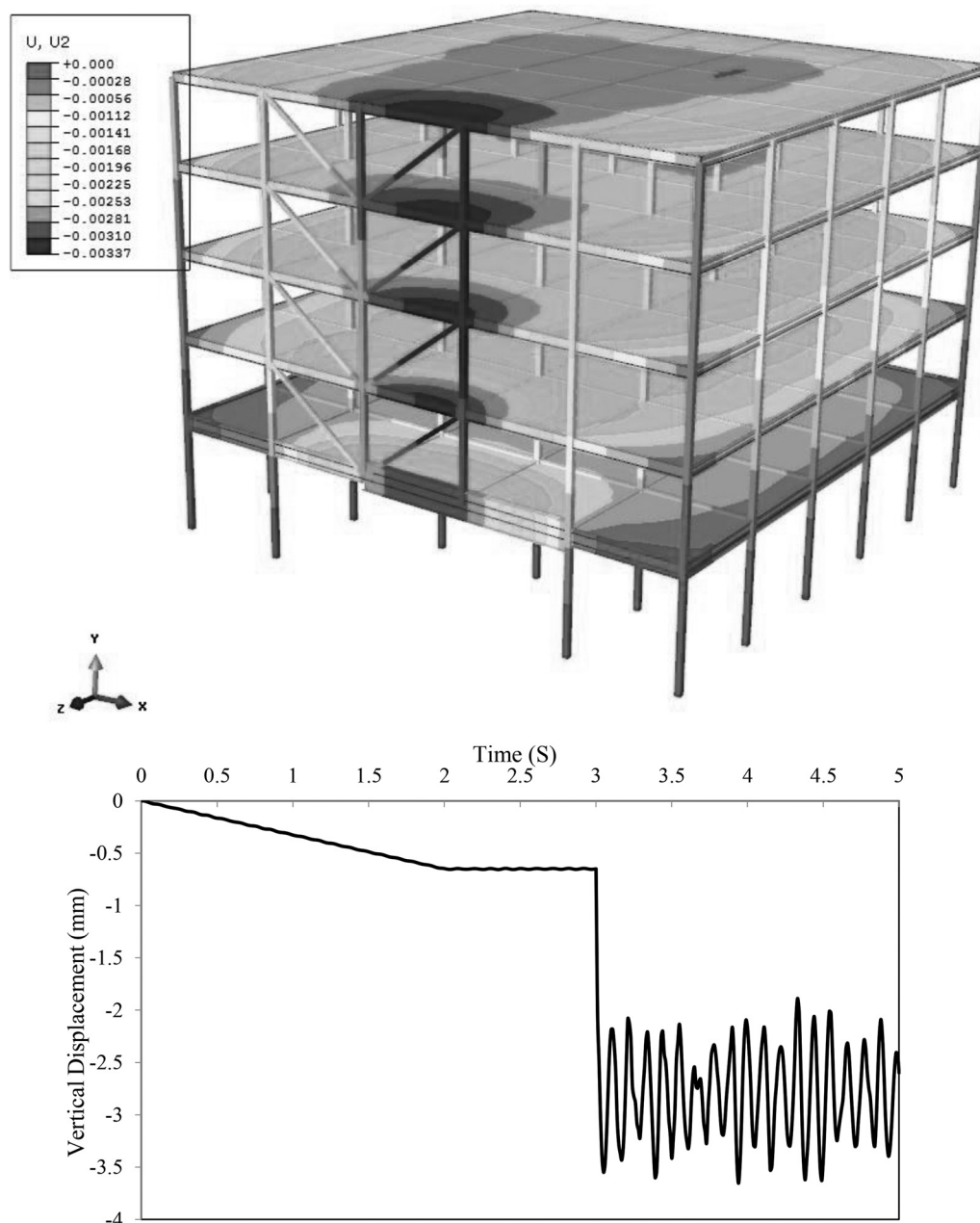
energy had to be absorbed by the rest of the structural elements. Therefore, a large force was exerted on the adjacent beam, which resulted in its rotation outside the plastic zone. According to the rotation criteria (Table 6), the rotation at the joint area exceeded 0.0304 radians.

10-Story Structure with Moment-Resisting Frames

As in the previous case (the five-story structure), when the column was suddenly removed (Fig. 12), the node above the removed column started to vibrate and reached a maximum displacement of 257 mm, eventually reaching a displacement of approximately 210 mm. Fig. 13 shows the history of displacement during the loading process. Upon removal of the column, the adjacent beams and columns, too, experienced severe axial load. As shown in Figs. 14 and 15, Columns D2 and B1, respectively, experienced the maximum force and the maximum rate of increase in the force. The rate of increase in B1 was 89%. Fig. 15 shows that the axial force of Beam B1-C1 rose by 46%. This increase and the deformation in the element caused the plastic rotation of the element, which exceeded the allowed quantity, as shown in Fig. 16.

Five-Story Building Equipped with CBFs above the Removed Column

In this part of the study, a five-story structure with steel moment-resisting frames was equipped with diagonal CBFs with square-box sections of 200 mm in width and 8 mm in thickness to manage the response of the structure. The displacement above the removed column in the structure equipped with diagonal CBFs, upon column removal, vibrated, which increased the displacement from 0.65 mm to a maximum of 3.65 mm (Fig. 17). Nonetheless, the maximum displacement caused by the removal of the column was far less than that in the absence of CBFs. As with the previous case, the beams and columns around the removed columns experienced a sudden rise in the axial forces, as shown in Figs. 18 and 19. Yet, this change was less than that in the absence of CBFs. With the removal of the column, a severe tension force was exerted on the CBFs, especially those of the first floor, which increased the force, from 44 to

© ASCE 04018025-11 Pract. Period. Struct. Des. Constr.

Pract. Period. Struct. Des. Constr., 2018, 23(4): 04018025

Fig. 17. Curve of the displacement above the removed column in the five-story structure equipped with diagonal CBFs.

143 kN, and converted the force from compressive to tensile, as shown in Fig. 20. A comparison of Figs. 18 and 12 shows that installing diagonal CBFs above the removed column led to little change in the axial force of the columns. However, it must be noted that there was a small rise in the force in columns on Axes B1 and B2 (at 10 and 2.7%, respectively) and a relative fall in other columns.

10-Story Building Equipped with Diagonal CBFs above the Removed Column
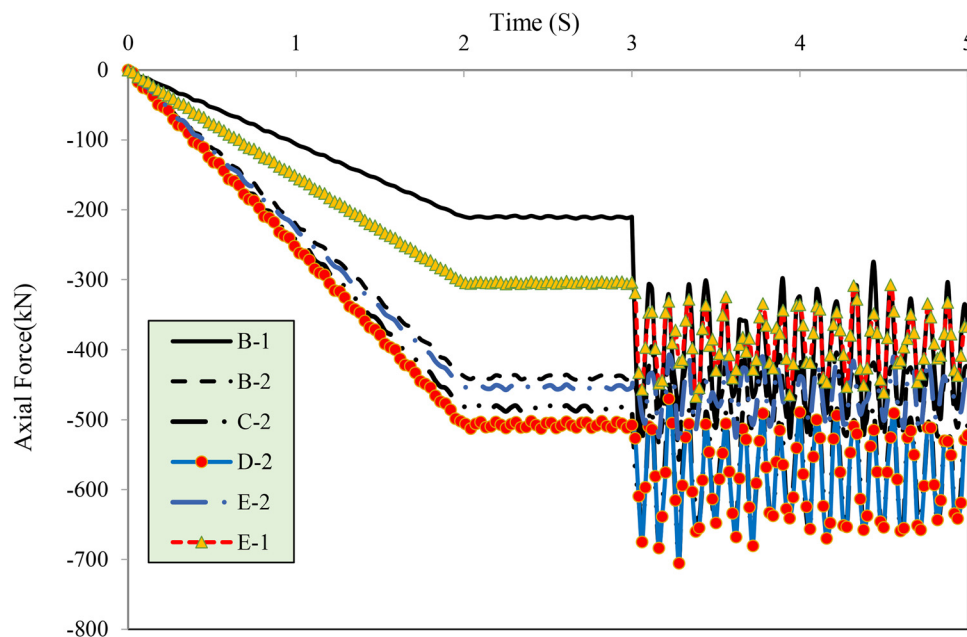
Upon removal of the column in the 10-story structure equipped with diagonal CBFs above the removed column, the displacement of the node above it rose and reached 4.5 mm (Fig. 21). As shown in Figs. 22 and 23, upon sudden removal of the column, the beams and columns around it experienced a sudden change in the axial force.

However, this change was insignificant compared with that in the absence of the CBFs. Only the axial force in Column B1 experienced a 5% growth compared with that in the absence of the CBFs. Also, the maximum tensile axial force (300 kN) was experienced in the CBFs on the first floor. Other CBFs had an insignificant role in the redistribution of loads, and little axial force was caused in them.
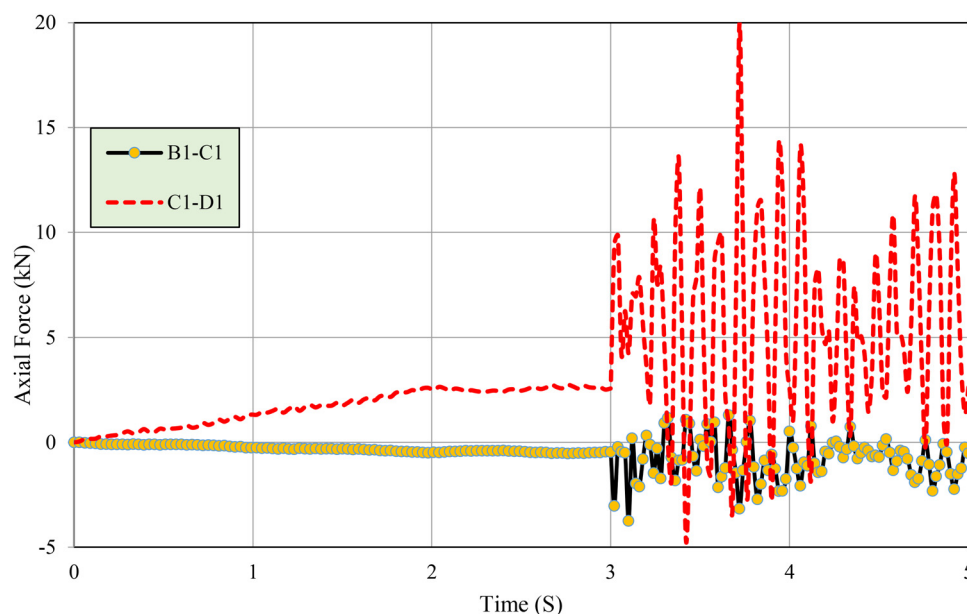
5- and 10-Story Structures Equipped with Cables

Because the cable system had an overall diameter of 100 mm, the maximum axial force that can be tolerated by all the cables was 1,295 kN. Figs. 24 and 25 show the displacement curves of the 5- and 10-story structures equipped with cable systems on the first and second floors, which indicate a fall in the deformation of the structural system compared with that of the unreinforced structure. The maximum displacements in the node above the removed column in

© ASCE 04018025-12 Pract. Period. Struct. Des. Constr.

Pract. Period. Struct. Des. Constr., 2018, 23(4): 04018025

Fig. 18. Curve of the internal axial force in the columns around the removed column on the ground floor.
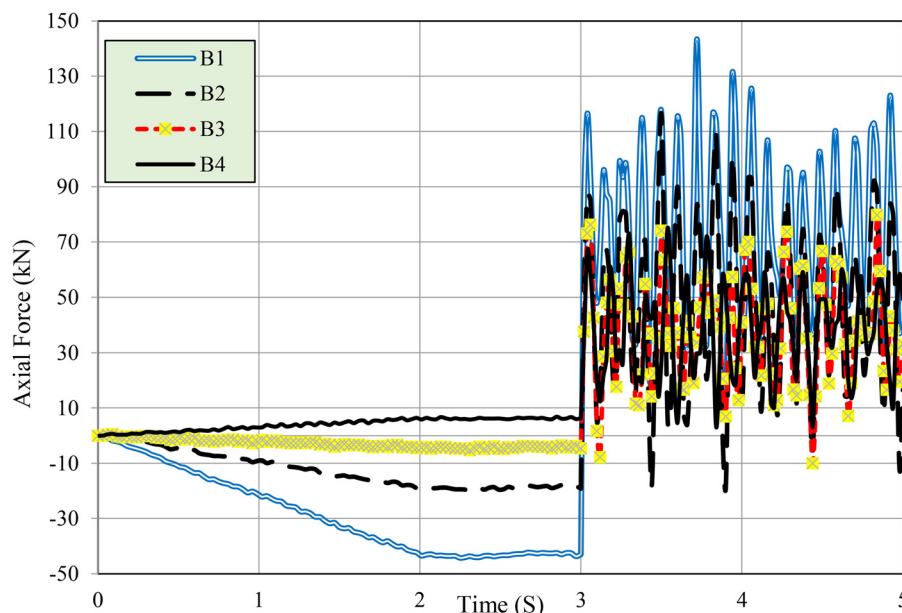

Fig. 19. History of the internal axial force in the columns around the removed column on the ground floor.
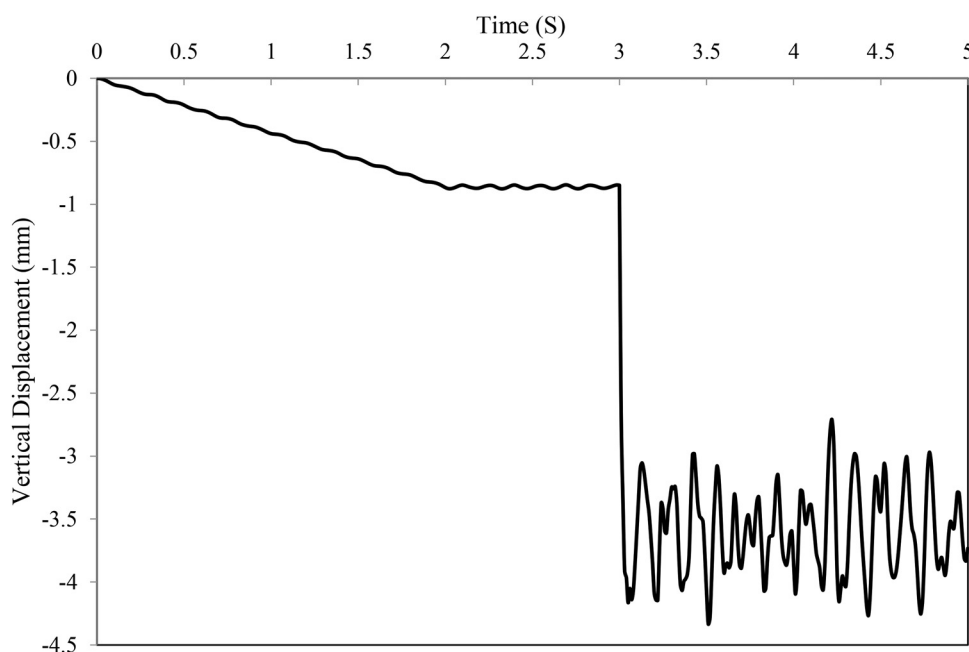
the 5- and 10-story structures were 6.69 and 10 mm, respectively. As shown in Figs. 26 and 27, the presence of the cables reduced the axial force compared with that in the absence of reinforcement. Also, in the five-story structure with cables (Fig. 28), Column B1 had the maximum rate of increase in the axial force (148%) after the removal of the column, and this column also demonstrated the highest sudden rise in force in previous models. In this system, all the structure elements remained elastic, and the structure collapse did not progress.

Based on the results of the analyses, it can be seen that in the unreinforced scenario, both in the low- and midrise structures, upon sudden removal of the column adjacent to the building

entrance, due to the rise in the influence area of loading, the adjacent beams experienced plasticity and exceeded the GSA (2013) plastic rotation criteria. Reinforcing the structure with diagonal CBFs above the span on the removed column succeeded in managing the structural response. At higher levels, it was not necessary to use CBFs of the same section as on the ground floor. The action of the catenary cables, installed on the same floor where the column was removed, succeeded in managing the structural response. The cables, with their chain action, managed to transfer the load path, assisted by the beam, to the adjacent columns. Also, the dynamic response of the beams and columns around the removed column tended to be of the same magnitude and

© ASCE 04018025-13 Pract. Period. Struct. Des. Constr.

Pract. Period. Struct. Des. Constr., 2018, 23(4): 04018025

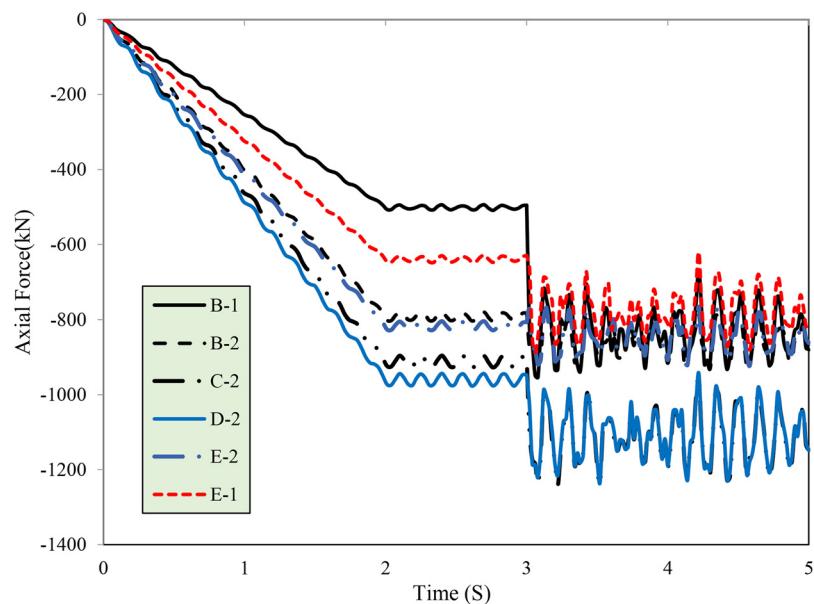**Fig. 20.** History of the internal axial force in CBFs.

Fig. 21. Curve of the displacement above the removed column in the 10-story structure equipped with CBFs.

behavior, which is because the structural grids of these two types of building were the same. Because the initially analyzed sections were designed based on (dead and live) gravitational loads and seismic design combination, most structural sections managed to act efficiently. However, if the structural sections had been designed only based on gravitational loads, with the removal of the column, most elements obviously would fail and yield because of the sudden energy exerted upon them. In this analysis, no columns experienced yield, and only the beams around the removed column entered the plastic phase in the unreinforced structures. Upon analysis of the stress caused in the columns at the end of the loading process, it could be seen that these columns experienced a stress of almost twice as much as that in the equation $1.2D + 0.5L$.

Concluding Remarks

In this study, 3D finite-element models, initially analyzed and designed in ETABS, for two structures with steel moment-resisting frames (5- and 10-story buildings) were developed in *Abaqus*. In all the models, the behavior of nonlinear geometry and materials were considered. First, two validity assessments were conducted with two experimental models to ensure the accuracy of the behavior of the models, lateral boundary, and constraints. Then, numerical results were presented and discussed. The results show that a more economical and reliable method is offered by 3D models. With this model, nonlinear dynamic analysis of the 5- and 10-story structures reinforced with either diagonal CBFs or cables was conducted, the results of which are outlined as follows:

© ASCE 04018025-14 Pract. Period. Struct. Des. Constr.

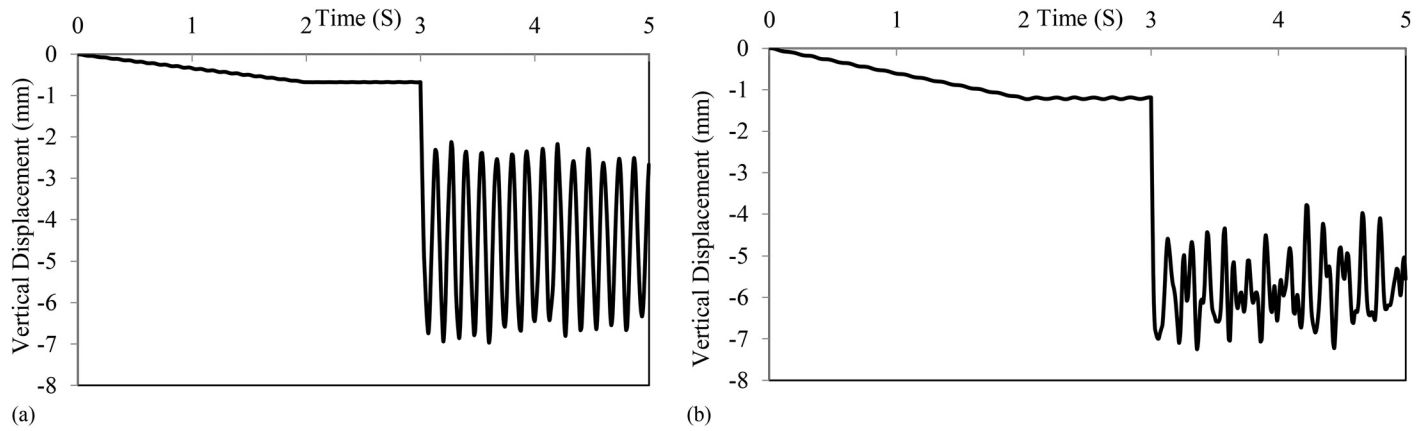Pract. Period. Struct. Des. Constr., 2018, 23(4): 04018025

Fig. 22. Curve of the internal axial force in the columns around the removed column on the ground floor.
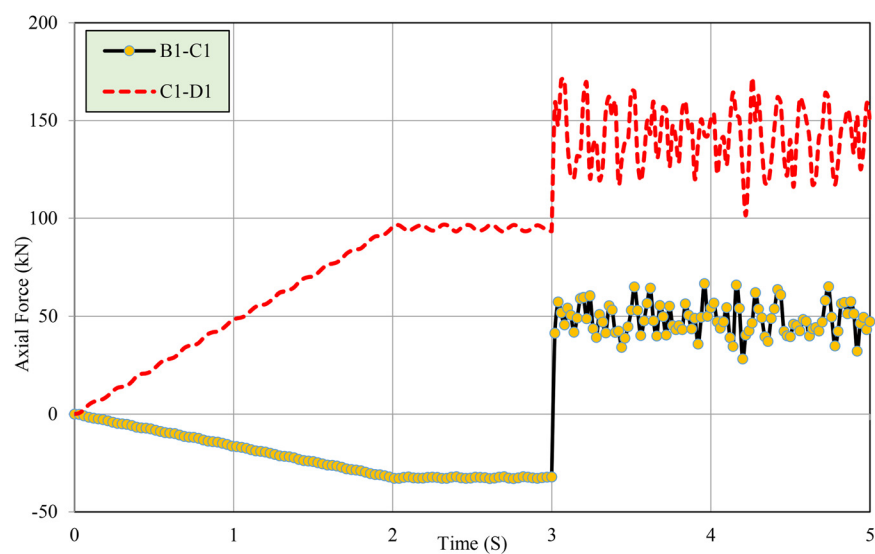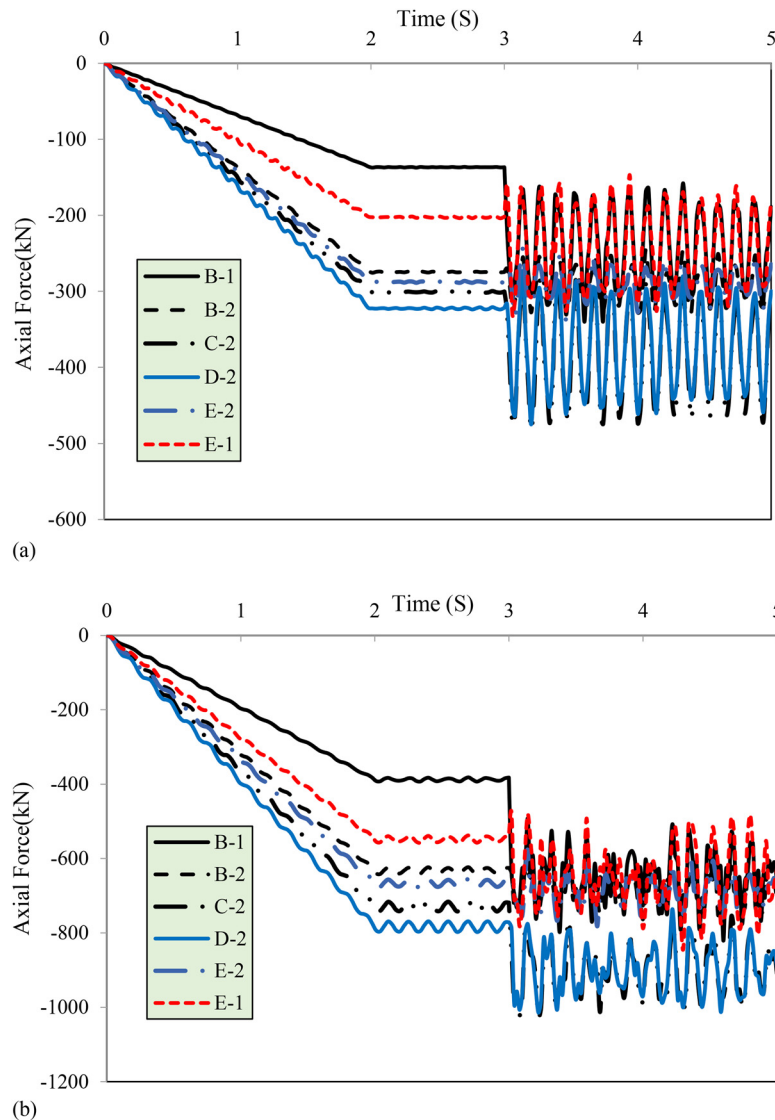

Fig. 23. History of the internal axial force in the columns around the removed column on the ground floor.
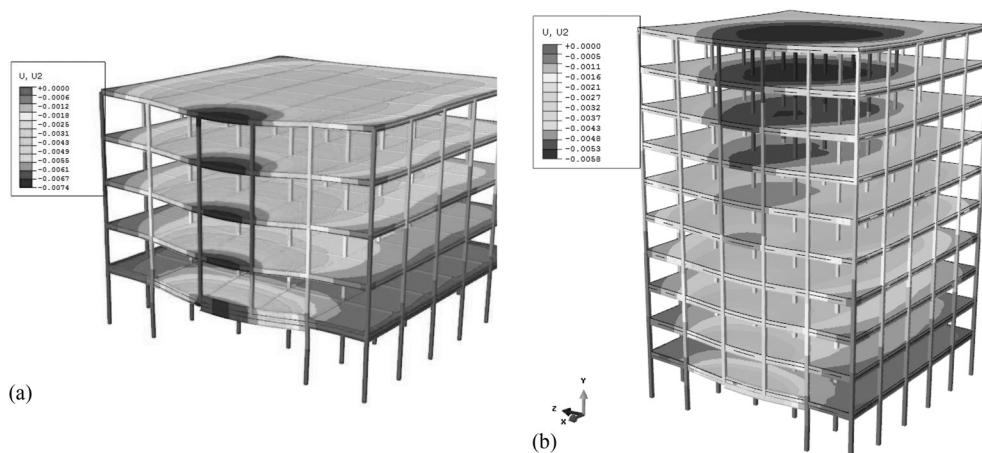
Fig. 24. Distribution of displacements along the *y*-axis (in meters): (a) 5-story structure; and (b) 10-story structure.

Fig. 25. Curves of displacement above the removed column in the structure equipped with cables: (a) 5-story structure; and (b) 10-story structure.
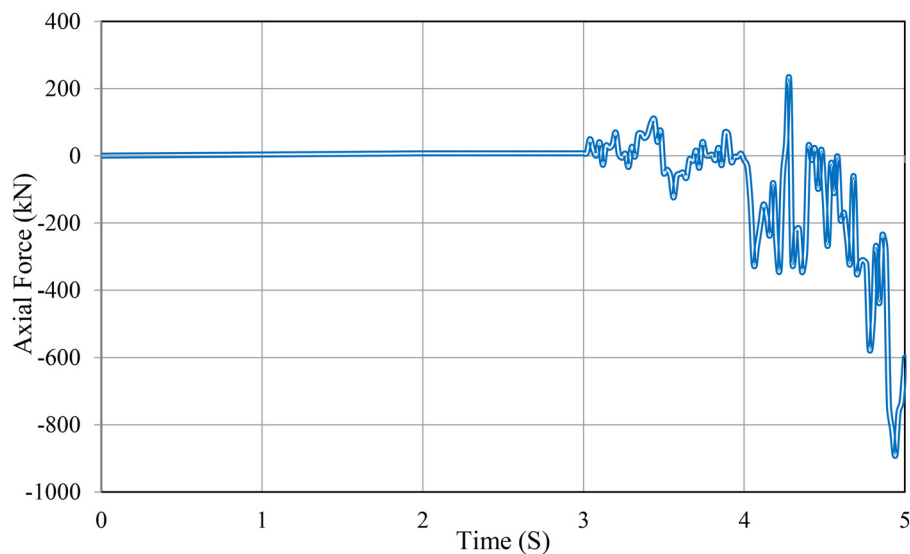

Fig. 26. Curves of internal axial forces in the columns around the removed column on the ground floor: (a) 5-story structure; and (b) 10-story structure.

- The dynamic responses of the beams and columns in both types of reinforced structures were similar to each other, which is directly linked to the influence area of loading.

- Structural systems designed based on gravitational loads and seismic design combination can respond efficiently to increased loads, but upon sudden removal of the column and the ensuing
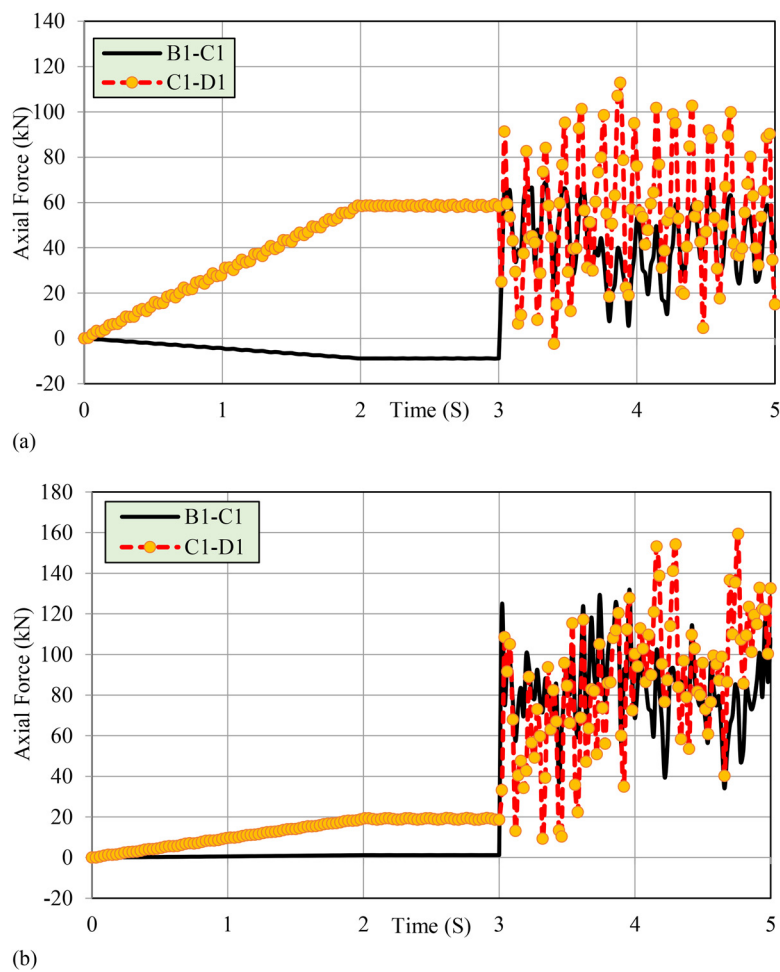
Fig. 27. History of internal axial forces in the columns around the removed column on the ground floor: (a) 5-story structure; and (b) 10-story structure.

Fig. 28. Curve of the internal axial force in the 5-story structure.

increase in plastic beam rotation, floor failure and collapse are inevitable.

- The presence of cables reduces the axial forces in beams and columns compared with those in the diagonal-CBF and no-reinforcement scenarios. These strong cables increase the

stiffness, resistance, and tolerance of the structure against progressive collapse. The cables provide an efficient alternative path for load transfer. The concrete slab of the floor and the elements of the frames with the cable act like a chain to manage the response of the structure.

- As a result of the tension in peripheral cables, the concrete slab of the floor can withstand in-plane compressive forces.
- Both reinforcement methods discussed, the use of cables and diagonal CBFs, can manage the structural response to the progressive collapse. Nonetheless, the use of cables is more efficient than CBFs connected to beams and frame nodes because of the cables' integrity with the diaphragm.
- The use of CBFs in 5- and 10-story structures led to a 98% fall in the displacement of the node above the removed column, compared with that of the unreinforced building at the same node, and the use of cables in 5- and 10-story structures led to a 98% and a 96% fall, respectively.

References

AISC (American Institute of Steel Construction). 2010. *Manual of steel construction, load and resistance factor design.* Chicago: AISC.

Andalib, Z., M. A. Kafi, A. Kheyroddin, and M. Bazzaz. 2014. "Experimental investigation of the ductility and performance of steel rings constructed from plates." *J. Constr. Steel Res.* 103: 77–88. https://doi.org/10.1016/j.jcsr.2014.07.016.

ASCE. 2010. *Minimum design loads for buildings and other structures.* Reston, VA: ASCE.

Bazzaz, M., Z. Andalib, M. A. Kafi, and A. Kheyroddin. 2015a. "Evaluating the performance of OBS-C-O in steel frames under monotonic load." *Earthquakes Struct.* 8 (3): 697–710. https://doi.org/10.12989/eas.2015.8.3.699.

Bazzaz, M., Z. Andalib, A. Kheyroddin, and M. A. Kafi. 2015b. "Numerical comparison of the seismic performance of steel rings in off-centre bracing system and diagonal bracing system." *Steel Compos. Struct.* 19 (4): 917–937. https://doi.org/10.12989/scs.2015.19.4.917.

Bazzaz, M., A. Kheyroddin, M. Kafi, and Z. Andalib. 2011. "Evaluating the performance of steel ring in special bracing frame." In *Proc., 6th Int. Conf. of Seismology and Earthquake Engineering.* Tehran, Iran: International Institute of Earthquake Engineering and Seismology.

Bazzaz, M., A. Kheyroddin, M. A. Kafi, and Z. Andalib. 2012a. "Evaluation of the seismic performance of off-centre bracing system with ductile element in steel frames." *Steel Compos. Struct.* 12 (5): 445–464. https://doi.org/10.12989/scs.2012.12.5.445.

Bazzaz, M., A. Kheyroddin, M. A. Kafi, and Z. Andalib. 2012b. *Modeling and analysis of steel ring devised in off-centric braced frame with the goal of improving ductility of bracing systems.* Tehran, Iran: Iran Scientific and Industrial Researches Organization.

Bazzaz, M., A. Kheyroddin, M. A. Kafi, Z. Andalib, and H. Esmaeili. 2014. "Seismic performance of off-centre bracing system with circular element in optimum place." *Int. J. Steel Struct.* 14 (2): 293–304. https://doi.org/10.1007/s13296-014-2009-x.

Bischoff, P. H., and S. H. Perry. 1991. "Compressive behaviour of concrete at high strain rates." *Mater. Struct.* 24 (6): 425–450. https://doi.org/10.1007/BF02472016.

DoD (Department of Defense). 2009. *Unified facilities criteria: Design of buildings to resist progressive collapse.* UFC 4-023-03. Washington, DC: DoD.

Ebadi Jamkhaneh, M., M. Ahmadi, and A. Kheyroddin. 2015. "Assessment and strengthening of special moment frame under progressive collapse." In *Proc., 3rd Int. Congress on Civil Engineering, Architecture and Urban Development.* Tehran, Iran: Shahid Beheshti Univ.

Elsanadedy, H. M., T. H. Almusallam, Y. R. Alharbi, Y. A. Al-Salloum, and H. Abbas. 2014. "Progressive collapse potential of a typical steel building due to blast attacks." *J. Constr. Steel Res.* 101: 143–157. https://doi.org/10.1016/j.jcsr.2014.05.005.

FIB (International Federation for Structural Concrete). 2008. *Constitutive modelling of high strength/high performance concrete. State-of-art report.* FIB Bulletin 42. Lausanne, Switzerland: FIB.

Fu, Q., B. Yang, Y. Hu, G. Xiong, S. Nie, W. Zhang, and G. Dai. 2016. "Dynamic analyses of bolted-angle steel joints against progressive collapse based on component-based model." *J. Constr. Steel Res.* 117: 161–174. https://doi.org/10.1016/j.jcsr.2015.10.010.

Galal, K., and T. El-Sawy. 2010. "Effect of retrofit strategies on mitigating progressive collapse of steel frame structures." *J. Constr. Steel Res.* 66 (4): 520–531. https://doi.org/10.1016/j.jcsr.2009.12.003.

Gerasimidis, S. 2014. "Analytical assessment of steel frames progressive collapse vulnerability to corner column loss." *J. Constr. Steel Res.* 95: 1–9. https://doi.org/10.1016/j.jcsr.2013.11.012.

Gerasimidis, S., and J. Sideri. 2016. "A new partial-distributed damage method for progressive collapse analysis of steel frames." *J. Constr. Steel Res.* 119: 233–245. https://doi.org/10.1016/j.jcsr.2015.12.012.

Grote, D. L., S. W. Park, and M. Zhou. 2001. "Dynamic behavior of concrete at high strain rates and pressures: I. experimental characterization." *Int. J. Impact Eng.* 25 (9): 869–886. https://doi.org/10.1016/S0734-743X(01)00020-3.

GSA (General Service Administration). 2013. *Alternate path analysis and design guidelines for progressive collapse resistance.* Washington, DC: GSA.

Homaioon Ebrahimi, A., P. Martinez-Vazquez, and C. C. Baniotopoulos. 2017. "Numerical studies on the effect of plan irregularities in the progressive collapse of steel structures." *Struct. Infrastruct. Eng.* 13 (12): 1576–1583. https://doi.org/10.1080/15732479.2017.1303842.

Hsu, L. S., and C. T. T. Hsu. 1994. "Complete stress-strain behaviour of high-strength concrete under compression." *Mag. Concr. Res.* 46 (169): 301–312. https://doi.org/10.1680/macr.1994.46.169.301.

Khandelwal, K., S. El-Tawil, and F. Sadek. 2009. "Progressive collapse analysis of seismically designed steel braced frames." *J. Constr. Steel Res.* 65 (3): 699–708. https://doi.org/10.1016/j.jcsr.2008.02.007.

Kim, H. S., J. Kim, and D. W. An. 2009. "Development of integrated system for progressive collapse analysis of building structures considering dynamic effects." *Adv. Eng. Softw.* 40 (1): 1–8. https://doi.org/10.1016/j.advengsoft.2008.03.011.

Kim, J., and T. Kim. 2009. "Assessment of progressive collapse-resisting capacity of steel moment frames." *J. Constr. Steel Res.* 65 (1): 169–179. https://doi.org/10.1016/j.jcsr.2008.03.020.

Kwasniewski, L. 2010. "Nonlinear dynamic simulations of progressive collapse for a multistory building." *Eng. Struct.* 32 (5): 1223–1235. https://doi.org/10.1016/j.engstruct.2009.12.048.

Lee, C. H., S. Kim, K. H. Han, and K. Lee. 2009. "Simplified nonlinear progressive collapse analysis of welded steel moment frames." *J. Constr. Steel Res.* 65 (5): 1130–1137. https://doi.org/10.1016/j.jcsr.2008.10.008.

Liu, J. L. 2010. "Preventing progressive collapse through strengthening beam-to-column connection, Part 1: Theoretical analysis." *J. Constr. Steel Res.* 66 (2): 229–237. https://doi.org/10.1016/j.jcsr.2009.09.006.

Malvar, L. J., and J. E. Crawford. 1998. *Dynamic increase factors for concrete.* Hueneme, CA: Naval Facilities Engineering Service Center Port.

Naji, A., and F. Irani. 2012. "Progressive collapse analysis of steel frames: Simplified procedure and explicit expression for dynamic increase factor." *Int. J. Steel Struct.* 12 (4): 537–549. https://doi.org/10.1007/s13296-012-4008-0.

Nayal, R., and H. A. Rasheed. 2006. "Tension stiffening model for concrete beams reinforced with steel and FRP bars." *J. Mater. Civ. Eng.* 18 (6): 831–841. https://doi.org/10.1061/(ASCE)0899-1561(2006)18:6(831).

Pirmoz, A., and M. M. Liu. 2016. "Finite element modeling and capacity analysis of post-tensioned steel frames against progressive collapse." *Eng. Struct.* 126: 446–456. https://doi.org/10.1016/j.engstruct.2016.08.005.

Rezvani, F. H., A. M. Yousefi, and H. R. Ronagh. 2015. "Effect of span length on progressive collapse behaviour of steel moment resisting frames." *Structures* 3: 81–89. https://doi.org/10.1016/j.istruc.2015.03.004.

Tan, S., and A. Astaneh-Asl. 2003. "Use of steel cables to prevent progressive collapse of existing buildings." In *Proc., Annual Meeting of the Los Angeles Tall Buildings Structural Design Council.* Los Angeles: Los Angeles Tall Buildings Structural Design Council.

Wang, X. L., X. Z. Lu, and L. P. Ye. 2007. "Numerical simulation for the hysteresis behavior of RC columns under cyclic loads." *Eng. Mech.* 24 (12): 76–81.

© ASCE 04018025-18 Pract. Period. Struct. Des. Constr.

Pract. Period. Struct. Des. Constr., 2018, 23(4): 04018025